A multi-scale modelling strategy to determine the effective elastic properties of *Pinus pinaster* (Ait.) accounting for variability

Romain Chevalier[1,2] · Marco Montemurro[1] · Régis Pommier[1] · Anita Catapano[1]

Abstract

Multi-scale numerical homogenisation strategies have been used in the recent years to efficiently compute the effective elastic properties of heterogeneous materials. Coupled with a stochastic approach, they can be applied to natural material such as wood to take into account the variability of their properties. In the case of *Pinus pinaster* (Ait.), available elastic properties are based on those of generic softwood species due to a lack of data in the literature, reducing the overall precision of the results. This paper proposes an efficient numerical framework based on both a general numerical homogenisation method and the well-known Monte Carlo approach to determine the equivalent elastic properties at the macroscopic scale, with the associated variability, of the *Pinus pinaster* (Ait.) species. The coherence of the numerical model is established by comparison with analytical and experimental results available in the literature. The obtained results reveal very good accuracy in terms of equivalent elastic properties with a macroscopic behaviour characterised by an orthotropic symmetry. Moreover, the influence of the distance from the pith on the equivalent macroscopic elastic response is highlighted.

✉ Marco Montemurro
marco.montemurro@ensam.eu

Romain Chevalier
romain.chevalier@u-bordeaux.fr

Régis Pommier
regis.pommier@u-bordeaux.fr

Anita Catapano
anita.catapano@bordeaux-inp.fr

[1] Université de Bordeaux, Arts et Métiers Institute of Technology, CNRS, INRA, Bordeaux INP, HESAM Université, I2M UMR 5295, F-33405 Talence, France

[2] Gascogne Bois, Route de Cap de Pin, 40210 Escource, France

Introduction

Wood is a natural material whose importance rose exponentially over the last few years. Indeed, this renewable material perfectly fits several "Sustainable Development Goals" set by the United Nations and is highly recommended by the IPCC's "Global Warming of 1.5 °C" report (IPCC 2018) as a solution to reduce carbon footprints in building and civil-engineering. In the South West of France, the current wood industry is particularly related to *Pinus pinaster* (Ait.), a softwood species indigenous of the South West of Europe, because of its vast presence across the whole area (between 75 and 84% of total forest area in two departments – Gironde and Landes (Sanz et al. 2020)). However, recent natural disasters caused important damages to the local *Pinus pinaster* (Ait.) population in these two French departments such as two storms, respectively Lothar and Martin in 1999 (24 millions m^3) and Klaus in 2009 (37 millions m^3) (Moreau 2010), and the forest fires of the last years and especially in 2022 (30790 hectares according to EFFIS's data). Additionally, IPCC's report (IPCC 2018) evokes that in Europe, "*Projected impacts on forests as climate change occurs include increases in the intensity of storms, wildfires and pest outbreaks (Settele et al., 2014), potentially leading to forest dieback (medium confidence)*". These events will lead to a scarcity of material sources as well as a modification in the ecophysiological response of *Pinus pinaster* (Ait.) (Niccoli et al. 2019; IPCC 2014). Thereby, it is of great importance to develop rigorous materials laws and models relying on *Pinus pinaster* (Ait.) properties conscientiously extracted from the scientific literature to obtain reliable results adapted to this local species and improve the material worth in the wood industry.

Several studies focus on the experimental mechanical characterisation of *Pinus pinaster* (Ait.) tempered at 12% humidity. Cariou (1987) presented elastic properties issued from tensile and shear tests on specimens visually chosen with a straight grain angle, constant spacing growth rings, high radius of curvature, and no presence of knots. Furthermore, he presented the results taken from Lahna (1983) obtained through compression tests. Xavier (2003) and Xavier et al. (2004, 2009) measured the shear mechanical properties from clear wood specimens extracted from a 74 years old *Pinus pinaster* (Ait.) tree. The properties are evaluated thanks to three different shear tests, the Iosipescu method, the off-axis method, and the Arcan method. Moreover, Santos et al. (2008) presented the results of tensile tests performed by Pereira (2005) to characterise the Young's moduli and the Poisson's ratios. Pereira et al. (2014) used an anisotropic-based method resting upon digital image correlation and tensile tests to evaluate elastic properties in the transverse plane of specimens. Finally, Santos (2007) determined the longitudinal Young's modulus, flexural modulus, and strength properties for several specimens of clear wood (with variability in density and growth ring width) through tensile and compression tests (parallel and transversal to the grain), shear tests, and flexural test.

Even though mechanical properties of *Pinus pinaster* (Ait.) are available in the scientific literature, a vast majority of studies still use approximate values or

classical softwood properties taken from Guitard (1987). Moreover, the variability as well as the intra-tree heterogeneity of wood properties and typology are also neglected. Indeed, wood is created by the division of the cambium, whose activity is impacted by several factors, such as climatic conditions, tree ageing, as well as silviculture, which affect geometrical, physical, and mechanical properties. Consequently, wood material is the result of the accumulation of several fluctuating layers alternating between earlywood (EW) and latewood (LW) which can be considered as a composite laminate with stochastic properties (Ghoroubi et al. 2022; Sun et al. 2022; Fabrizio et al. 2023; Chen et al. 2023).

Several analytical models, more or less sophisticated, have been developed to give an estimation of the elastic properties of heterogeneous materials in the presence of variability. They are based on empirical and semi-empirical formulæ including simplifying assumptions, such as the models presented by Einstein (1905) and by Hashin and Shtrikman (1962b). Several studies based on numerical approaches on the same topic are also available in the scientific literature. McManus (1993) proposed a probabilistic method to calculate equivalent elastic properties based on standard classical laminated plate theory (CLPT) relation, while Alazwari and Rao (2019), using the same CLPT relations, compared the results of the probabilistic approach with an interval approach.

At lower scales, different homogenisation techniques are available in the literature. For example, Catapano and Jumel (2015) used a numerical homogenisation method based on the strain energy density of periodic media to determine the equivalent elastic properties of polymers reinforced with inclusions as well as their macroscopic elastic symmetry class. This technique has also been employed by Delucia et al. (2020) to determine the properties of cork-based composites coupled with a Monte-Carlo method to take into consideration the variability of this natural material.

In the case of wood, Ŝejnoha et al. (2019) used analytical and numerical methods on units cell of spruce wood to determine thermo-hygro-mechanical properties of the EW and LW phases. The local micro-structure was obtained thanks to X-ray computational micro-tomography. Girardon et al. (2016) proposed a parametric model describing the influence of cambial age on the effective properties of poplar laminated veneer lumber by using the analytical formulæ of Reuss-Voigt, (Reuss 1929; Voigt 1889), and the Steiner's principle coupled with a stochastic approach. In Hofstetter et al. (2005) a four-step homogenization scheme has been proposed which goes from the scale of nanometers (i.e., the one of hemicellulose, lignin, etc.) up to the scale of millimeters (i.e., the one of the wood rings). In Qing and Mishnaevsky (2010) the model proposed by Hofstetter et al. (2005) was exploited to propose a 3D micromechanical semi-analytical model of softwood. An improved rule-of-mixture model, based on 3D stress–strain relations was proposed. The improved rule of mixture model (IRoM) was compared with the classical rule-of-mixture (RoM) and finite element (FE) simulations. In Saavedra Flores et al. (2016) the previous works of Hofstetter et al. (2005) and Qing and Mishnaevsky (2010) were generalised up to the scale of cross-laminated timber structures in order to better investigate the rolling shear failure of this specific class of composite laminates.

The main goal of this paper is to propose a numerical framework based on a multi-scale FE model capable of evaluating the elastic properties of a specific softwood species, i.e., the *Pinus pinaster* (Ait.), accounting for its variability. Unlike the works cited above, in this paper, a two-step homogenisation scheme is proposed taking into account the very limited amount of data available in literature on *Pinus pinaster* (Ait.). Firstly, at a length scale of hundreds of micrometres (no data in terms of elastic properties are available at lower scales for *Pinus pinaster* (Ait.)), EW and LW properties resting on experimental data, taken from the scientific literature are homogenised at the scale of the tree rings through a parametric analytical model. Then, at a length scale of millimetres, the macroscopic equivalent elastic behaviour of small samples of *Pinus pinaster* (Ait.) are computed through a numerical homogenisation procedure.

In the latter case, the multi-scale homogenisation method presented in Catapano and Jumel (2015) and Delucia et al. (2020) has been adapted to the 3D FE model of a representative volume element (RVE) of wood specimens extracted from several positions in a "synthetic" log specially developed in the context of this work. The model takes into consideration the heterogeneity and variability of main wood properties at the microscopic scale (intra-ring) and at the mesoscopic scale (inter-rings). The homogenisation procedure is then coupled with a stochastic approach, i.e., the Monte-Carlo method, to efficiently compute the related variability. The results are compared with the available experimental data in the scientific literature to evaluate the accuracy of the model.

The paper is organised as follows. The procedure to proficiently model synthetic *Pinus pinaster* (Ait.) logs is presented in the sect. Generation of a synthetic log of *Pinus pinaster* (Ait.). The section Elastic properties of *Pinus pinaster* (Ait.) early and latewood at the microscopic scale is dedicated to the determination of growth rings` mechanical properties taking into consideration the variability induced by the geometrical and physical parameters of the logs. The numerical homogenisation method as well as the related 3D FE-model are discussed in the sect. Determination of the elastic properties at the macroscopic scale. The numerical results are illustrated and discussed in the sect. Numerical results at the macroscopic scale accounting for variability. Finally, conclusions and prospects are drawn in the sect. Conclusion.

Generation of a synthetic log of *Pinus pinaster (Ait.)*

A local cylindrical coordinate system is used to describe wood properties defined by three planes of orthogonal symmetry, as shown in Fig. 1: longitudinal direction L, radial direction R corresponding to the diametrical growth direction, and tangential direction T to the annual growth rings. Three planes can be identified in this system: the transverse plane RT, the radial longitudinal plane LR and the tangential longitudinal plane LT.

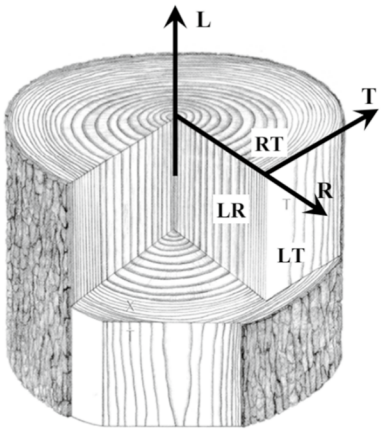

Fig. 1 Local cylindrical reference system, (Moutee 2006)

Definition of the problem scales

Wood is a highly heterogeneous and anisotropic natural composite whose structure can be defined at several working scales:

- Microscopic scale: growth rings constituted by the accumulation of wood cells (90% of longitudinal tracheids) and produced by the cambium.
- Mesoscopic scale: elementary volumes emerging from the alternation of growth rings and considered as lamellar composites. Each ring can be decomposed in EW and LW regions.
- Macroscopic scale: wood logs composed by concentric growth rings and produced by the cambium as radial growth.

Hypotheses at the basis of the numerical model of the wood log

The proposed model aims at numerically reproducing, at several scales, semi-realistic natural logs of *Pinus pinaster* (Ait.) considering simplifying hypotheses to reduce the overall complexity of the problem and according to the existing data available in the scientific literature. The following hypotheses are made to build the numerical model of the wood log:

1. The synthetic trunk will be considered as a perfect cylinder with a centred pith. Hence, the influence of external factors such as light, gravity, and wind are neglected;
2. The variability in the longitudinal direction (direction of the stem) of wood properties due to conic angle, grain angle, and proximity of living crown, is disregarded;
3. The log is considered free of reaction wood (Plomion et al. 2000);

4. The influence of micro-fibrils angle (MFA) on the effective properties is neglected as there is too few information concerning *Pinus pinaster* (Ait.) on the evolution of MFA with cambial age (local data available in Brémaud et al. (2013));
5. The presence of defects such as knots and resin pockets is neglected (Moreau 2010);
6. The formation of heartwood, a physiological phenomenon transforming living cells of sapwood into dead heartwood cells (see Kokutse et al. 1999; Taylor et al. 2002), is not taken into consideration. Indeed, Berthier et al. (2001) showed no true mechanical differences between sapwood and heartwood in the case of *Pinus pinaster* (Ait.);
7. Growth rings are supposed concentric to the pith. Moreover, they are considered composed of two phases, i.e. EW and LW, because of the abrupt transition between their respective densities for *Pinus pinaster* (Ait.), as discussed in Moreau (2010) and Chevalier et al. (2024). The differentiation arises because of variations between water demand and availability during growing seasons. The probability of formation of false rings is considered null.

An additional assumption is made for the wood formed during the first years of cambial activity. It is called juvenile wood (Zobel and Sprague 1998), it shows specific properties and it has to be taken into consideration in the model. The modelling of juvenile and adult wood is dealt with by evaluating their influence on physical properties. The usual transition from juvenile to adult wood is estimated at 12 years, as presented by Moreau (2010) and will be considered over 15 years in this study.

Four parameters, i.e., rings widths, EW/LW volume ratio in each ring, ring mean densities, and LW densities allow to model the synthetic logs. Properties are supposed discretised according to ring number from pith to the bark.

To compare the parametric analytical model presented in the following subsections with existing data from the scientific literature, the reader is addressed to the work by Louzada (2003), who presented similar parameters expressed as mean values and coefficients of variation from pith to the corresponding cambial age studied for a population of *Pinus pinaster* (Ait.).

Variability description

In analogy with the work by Delucia et al. (2020) on the multi-scale modelling of cork agglomerates, the wood properties defined in this study are affected by uncertainty and their variability is described by a normal distribution defined at each ring number i (except the first two rings because of the lack of information in the scientific literature). For a generic property q_i, the normal probability density function $\psi(q_i)$ can be defined as:

$$\psi(q_i) := \frac{1}{\xi(q_i)\sqrt{2\pi}} \exp\left(-\frac{(q_i-\mu(q_i))^2}{2\xi(q_i)^2}\right), \tag{1}$$

Table 1 *Pinus pinaster* (Ait.) ring width mean values and variations at given cambial age taken from the literature

Sources	Cambial age [years]	RW (mm)	C_v(RW)(%)	Range of values (mm)
Louzada (2003)	6	7.34	15.2	4.50−10.80
Louzada (2003)	10	5.86	14.2	3.50−8.80
Louzada (2003)	13	5.13	14.2	3.10−7.80
Gaspar et al. (2008)	17	4.224	21.33	2.5−8.6

where $\mu(q_i)$ and $\xi(q_i)$ are the mean value and the standard deviation of the distribution of the property q_i, respectively. The mean value $\mu(q_i)$, standard deviation $\xi(q_i)$, and coefficient of variation $C_v(q_i)$ [%] can be expressed as follows:

$$\begin{aligned} \mu(q_i) &:= \tfrac{1}{N_v} \textstyle\sum_{j=1}^{N_v} q_{i,j}\,, \\ \xi(q_i) &:= \sqrt{\mu\Big(\big(q_i - \mu(q_i)\big)^2\Big)}\,, \\ C_v(q_i) &:= 100\tfrac{\xi(q_i)}{\mu(q_i)}, \end{aligned} \tag{2}$$

where $q_{i,j}$ is the j-th value of q_i occurring for N_v values.

Annual growth ring width

In the case of *Pinus pinaster* (Ait.), except for the firsts rings (2*nd* to 5*th*), ring width decreases with the number of rings. The decrease is faster at the transition between juvenile and adult wood. One can define, for a ring number i, an associated ring width RW_i. The numerical model proposed in this paper is based on the data obtained by Gaspar et al. (2008) and Nicholls et al. (1963) where a maximum RW_i is obtained at the 4-th ring ($\mathrm{RW}_4 \in [7, 11]$ mm) followed by a steep reduction until the limit of juvenile wood wherein $\mathrm{RW}_i = 2$ mm. Equation (3) gives the mean value of RW_i in [mm] chosen for the proposed model according to the ring number:

$$\mathrm{RW}_i = \begin{cases} \{2.5, 9.4, 10.0, 10.2, 10.1, 9.9, 9.0, 7.8, 6.5, 5.3, 4.3, 3.4, 2.8, 2.3\} \\ \qquad \text{for } i = 1, ..., 14, \\ 2 \text{ for } i \geq 15. \end{cases} \tag{3}$$

For each ring number, the coefficient of variation $C_v(\mathrm{RW}_i)$ is considered equal to 20% according to Gaspar et al. (2008) and Louzada (2003) who presented results for the evolution of RW from pith to bark for *Pinus pinaster* (Ait.), see Table 1. Table 1 reports the mean RW, the $C_v(\mathrm{RW}_i)$ and the range of values of RW for trees at several ages at a constant measure height. Considering $i = 2, ..., 15$, $C_v(\mathrm{RW}_i)$ equal to 20% is assumed.

Table 2 Mean diameter and standard deviation for wood logs taken from GB samples (149727 logs) and those of the proposed numerical model (100000 tests)

	GB sample	Numerical model
Mean diameter [mm]	313.1	313.6
Standard deviation [mm]	19.15	21.20

Tree age

In the Landes of Gascogne, 92% of the local forests are private lands. Hence, traceability of stands processed by Gascogne Bois (GB) company[1] is not ensured and tree ages are unknown. GB company possesses dendrological data on the mean and standard deviation of logs diameter evaluated on 149727 logs. The measurements were performed on logs of 2.5 m length extracted from tree trunks at heights belonging to the range [0, 8] m. It is noteworthy that GB standard deviation results are overvalued because referenced as 120 stacks of around 1250 trees. Few information exists on the trees processed by GB including a minimal age of 40 years old with the possibility to reach 60 years old. The proposed model has to take into consideration the heterogeneity of tree ages resulting in a varying number of rings. To this end, a hypothesis is introduced: in the following of this paper, a normal distribution with a mean age of 45.6 and a standard deviation of 4.52 is assumed (tree ages outside of the range [40, 62] years old are neglected). The aforementioned parameters, i.e., annual growth ring widths and tree ages, enable to propose geometric parameters for the numerical logs, which can be compared to the GB sample in terms of mean and standard deviation of the logs diameter, assuming a normal distribution, as reported in Table 2.

Latewood proportion

The latewood proportion (LWP) in growth rings is not constant. To the authors' knowledge, only Nicholls et al. (1963) present the evolution of LWP volume fraction with cambial age for *Pinus pinaster* (Ait.): it shows a global increase of LWP in juvenile wood before reaching a constant level in the adult zone. In the juvenile wood, the following hypothesis is introduced: the LWP linearly increases with ring number i, for $i = 2, 3, ..., 15$.

The mean LWP_i can be expressed as follows (Nicholls et al. 1963):

$$\mathrm{LWP}_i = \begin{cases} 0.08 \text{ for } i = 1, \\ 0.08 + 0.02(i-2) \text{ for } i = 2, ..., 15, \\ 0.36 \text{ for } i \geq 16. \end{cases} \tag{4}$$

[1] https://www.gascognebois.com/

with:

$$\mathrm{LWP}_i = \frac{R_{\mathrm{ext},i} - R_{\mathrm{LW}i}}{\mathrm{RW}_i}\,. \tag{5}$$

For each i−th ring, the coefficient of variation of LWP, $C_v(\mathrm{LWP}_i)$, is evaluated according to Gaspar et al. (2008) who observed a $C_v(\mathrm{LWP}_i)$ equal to 44.31% for 17 years old *Pinus pinaster* (Ait.). Considering $i = 2, ..., 15$, a $C_v\left(\mathrm{LWP}_i\right)$ equal to 40% is assumed.

Mean earlywood and latewood densities

The air dry density ρ is defined as the ratio of mass to volume of wood conditioned at a moisture content of 12% (i.e., mean relative density W_d). W_d can be defined as follows:

$$W_d = \frac{\rho}{\rho_w}, \tag{6}$$

where $\rho_w = 1000\ \mathrm{kg.m^{-3}}$ is the water density.

Similarly to the LWP, a linear evolution of W_d and LW densities, i.e. LW_d, with respect to the ring number, before reaching a limit value in the adult zone is considered. While Nicholls et al. (1963) provided the evolution of W_d with ring number, Moreau (2010) supplied LW_d for an extensive range of RW (varying from 1 to 11 mm) according to cambial age.

Equations (7) give $W_{d,i}$ and $\mathrm{LW}_{d,i}$ as function of the ring number. These relations are quantitatively extracted from the work by Nicholls et al. (1963) and Moreau (2010) and they will be used in the present study to model the wood densities.

$$W_{d,i} = \begin{cases} 0.43 \text{ for } i = 1, \\ 0.43 + \frac{0.12}{14}(i-2) \text{ for } i = 2, 3, ..., 15, \\ 0.55 \text{ for } i \geq 16. \end{cases} \tag{7a}$$

$$\mathrm{LW}_{d,i} = \begin{cases} 0.56 \text{ for } i = 1, \\ 0.56 + 0.01(i-2) \text{ for } i = 2, 3, ..., 15, \\ 0.70 \text{ for } i \geq 16. \end{cases} \tag{7b}$$

In the case of softwoods, it is well documented (Jodin and Militon 1994) that there is an inverse correlation between rings width and densities. Indeed, the quantity of wood produced by cambium during a growing season depends on climatic conditions, genetics, silviculture, and externals interactions (i.e. wind, snow). In the present work, the mass of EW and LW produced by a ring per year is considered constant and expressed as:

$$
\begin{aligned}
&S_i W_{d,i} = c_1 \iff \pi({R_{\text{ext},i}}^2 - {R_{\text{int},i}}^2) W_{d,i} = c_1, \\
&S_{\text{LW}i}\text{LW}_{d,i} = c_2 \iff \pi({R_{\text{ext},i}}^2 - {R_{\text{LW},i}}^2)\text{LW}_{d,i} = c_2,
\end{aligned} \tag{8}
$$

where S_i is the total ring surface, $S_{\text{LW}i}$ is the LW surface, $R_{\text{int},i}$, $R_{\text{ext},i}$, and $R_{\text{LW},i}$ are the internal and external radius of the ring, and internal radius of the LW part of the ring, respectively, while c_i $(i = 1, 2)$ are suitable constants. Therefore, according to Eqs. (7) and (8), evolutions of RW_i and LWP_i values induce a variation of the densities values as well, i.e., $W_{d,i} = W_{d,i}\left(\text{RW}_i, \text{LWP}_i\right)$, $\text{LW}_{d,i} = \text{LW}_{d,i}\left(\text{RW}_i, \text{LWP}_i\right)$.

Elastic properties of *Pinus pinaster (Ait.)* early and latewood at the microscopic scale

EW and LW elastic behaviour can be modelled through Hooke's law whose compliance matrix $\mathbf{S}$ is uniquely defined via 9 independent elastic constants, i.e., three Young's moduli $E_{m,k}$ $(m = L, R, T$ and $k = \text{EW}, \text{LW})$, three shear moduli $G_{mn,k}$ $(m, n = L, R, T,\ m \neq n,$ and $k = \text{EW}, \text{LW})$, and three Poisson's ratios $\nu_{mn,k}$ $(m, n = L, R, T, m \neq n,$ and $k = \text{EW}, \text{LW})$:

$$
\begin{Bmatrix} \varepsilon_L \\ \varepsilon_R \\ \varepsilon_T \\ \gamma_{LR} \\ \gamma_{TL} \\ \gamma_{RT} \end{Bmatrix} = \begin{bmatrix} \frac{1}{E_{L,k}} & \frac{-\nu_{RL,k}}{E_{R,k}} & \frac{-\nu_{TL,k}}{E_{T,k}} & 0 & 0 & 0 \\ \frac{-\nu_{LR,k}}{E_{L,k}} & \frac{1}{E_{R,k}} & \frac{-\nu_{TR,k}}{E_{T,k}} & 0 & 0 & 0 \\ \frac{-\nu_{LT,k}}{E_{L,k}} & \frac{-\nu_{RT,k}}{E_{R,k}} & \frac{1}{E_{T,k}} & 0 & 0 & 0 \\ 0 & 0 & 0 & \frac{1}{G_{LR,k}} & 0 & 0 \\ 0 & 0 & 0 & 0 & \frac{1}{G_{TL,k}} & 0 \\ 0 & 0 & 0 & 0 & 0 & \frac{1}{G_{RT,k}} \end{bmatrix} \begin{Bmatrix} \sigma_L \\ \sigma_R \\ \sigma_T \\ \tau_{LR} \\ \tau_{TL} \\ \tau_{RT}. \end{Bmatrix}, \tag{9}
$$

where ε_m and σ_m are the normal strain and stress, whilst γ_{mn} and τ_{mn} are the shear strain and stress, respectively.

In the scientific literature, wood elastic properties can be expressed as a linear function of the relative density, as described by Kasal (2004). Guitard (1987) proposed a linear model to compute softwoods elastic properties relative to mean density based on experimental results on a large variety of species, which is frequently used in most studies. Nonetheless, while this model is fairly accurate for lower relative densities, it looses in precision in the case of a high density softwood such as *Pinus pinaster* (Ait.). As the model proposed in this study considers each ring as constituted of an EW phase of low relative density and a LW phase of high relative density, the classical softwood model of Guitard (1987) is not adequate for the proposed model, and other sources have to be used to characterise the elastic behaviour of the EW and LW phases. Specifically, data relative to *Pinus pinaster* (Ait.) mechanical properties taken from the scientific literature are used to establish relationships that accurately describe the behaviour of this softwood species EW and LW, while taking into consideration the dependency on density. To this end, a linear relationship of the Young's and shear moduli with relative density is assumed, similarly to (Guitard (1987). Regarding the Poisson's ratios, there is not enough

Table 3 Macroscopic longitudinal Young's modulus and density obtained through flexural tests in Santos (2007) for *Pinus pinaster (Ait.)*

W_d	0.46	0.60	0.635	0.64	0.65	0.693	0.705	0.715	0.725
E_L [MPa]	13200	15700	16110	16600	16435	16794	17775	17100	17545

information in the case of *Pinus pinaster* (Ait.) and their values are considered constant. Since only few works describing the mechanical properties of the EW and LW phases are available in the literature (Cramer et al. 2005; Sejnoha et al. 2019), which are not related to *Pinus pinaster* (Ait.) species, a similar behaviour in terms of relative density between mean wood and EW/LW phases properties has been considered in this paper. Thereby, elastic laws describing the mechanical properties of *Pinus pinaster)* (Ait.) relative to W_d extracted from scientific literature data will be applied to the EW and LW phases of each ring.

Young's moduli

To the best of the authors' knowledge, no exhaustive models describing the trend of Young's moduli vs. the relative density for the specific softwood species of *Pinus pinaster* (Ait.) are available in the literature. Moreover, existing literature, such as Hofstetter et al. (2005), cannot unfortunately be exploited in this paper since they refer to generic softwood species. Nonetheless, specific data are available in several references for given densities such as Pereira (2005) (referenced in (Santos et al. 2008)), Cariou (1987); Santos (2007) and Gaspar et al. (2008). This information is exploited to establish a model adapted to Young's moduli of *Pinus pinaster* (Ait.), which will be extented to the EW and LW phases. In the case of the longitudinal Young's modulus, Santos (2007) provided nine values which are reported in Table 3 linking longitudinal Young's modulus to W_d for *Pinus pinaster* (Ait.).

Data provided in Table 3 show a linear relationship between the longitudinal modulus E_L [MPa] and relative density W_d. This linear relation can be formulated through Eq. (10) where a coefficient of determination ${R_d}^2 = 0.9581$ is adopted to fit data of Table 3.

$$E_L = 5874.4 + 16209 W_d. \tag{10}$$

These data can also be used to clarify the important difference between mechanical properties of *Pinus pinaster* (Ait.) and other softwood species. A comparison is provided in Fig. 2 between *Pinus pinaster* (Ait.) longitudinal modulus from Eq.(10) and the one of other softwood species extracted from Guitard (1987) as function of relative density.

To evaluate the other Young's moduli, E_R and E_T as a function of W_d, Cariou (1987), Pereira (2005) and Lahna (1983) experimental data are exploited. Since in the above works the estimated Young's moduli for a given relative density are not provided, the linear relationship of Eq. (10) has been used to assess the relative density associated

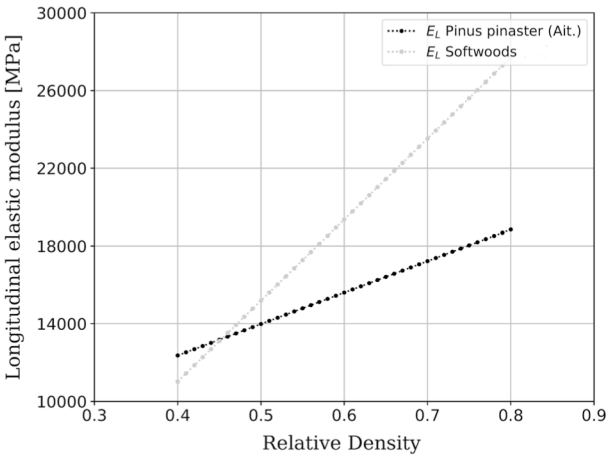

Fig. 2 Longitudinal Young's modulus of *Pinus pinaster* (Ait.) and other softwoods (Guitard 1987)

Table 4 Macroscopic Young's moduli and relative densities in Cariou (1987); Pereira (2005); and Lahna (1983) with estimated densities measured at a relative humidity of about 12%, *Pinus pinaster* (Ait.)

Sources	E_L (MPa)	E_R (MPa)	E_T (MPa)	W_d
Cariou (1987)	11369	–	703	0.3390
Pereira (2005)	15100	1910	1010	0.5690
Lahna (1983)	16140	2086	–	0.6439

with Young's moduli taken from these references. The estimated densities and the relative Young's moduli are reported in Table 4.

To generate the parametric analytical model at the scale of EW and LW phases, the linear relationships between Young's moduli and W_d are exploited. Indeed, since no specific law is available for elastic properties of EW and LW phases in the case of *Pinus pinaster* (Ait.), the linear regressions with relative density of Young's moduli (in MPa), associated with the phase $k = \mathrm{EW_d}, \mathrm{LW_d}$ are adopted:

$$\begin{aligned} E_{L,k} &= 16209k + 5874.4, \\ E_{R,k} &= 2743.1k + 319.98, \\ E_{T,k} &= 1333.7k + 250.88. \end{aligned} \tag{11}$$

The only difference between EW and LW phases is the relative wood density. In Eq. (11), $k = \mathrm{EW_d}, \mathrm{LW_d}$ is evaluated through Eqs. (7a)-(7b) and (8).

Table 5 *Pinus pinaster* (Ait.) Poisson's ratio (Cariou 1987) with k =EW,LW

$\nu_{RT,k}$	$\nu_{TL,k}$	$\nu_{RL,k}$
0.58	0.03	0.04

Shear moduli

Xavier et al. (2004) characterised the shear moduli of *Pinus pinaster* (Ait.) by carrying out two shear test methods, i.e., Iosipescu and off-axis. The relationships proposed to link shear moduli in MPa with infra-density (IF) (FPL–Forest Products Laboratory 2010) read:

$$G_{RT,k} = 495\mathrm{IF}_k, \quad G_{TL,k} = 2072\mathrm{IF}_k, \quad G_{LR,k} = 2402\mathrm{IF}_k, \tag{12}$$

with $\mathrm{IF}_k = \frac{W_{d,k}}{1.12+0.159W_{d,k}}$. The above formulæ are considered applicable to the densities examined in this study and will be applied to EW and LW phases.

Poisson's ratios

Cariou (1987) characterised the elastic properties of *Pinus pinaster* (Ait.) through experimental tests. Table 5 presents the Poisson's ratios obtained in (Cariou (1987). According to Bartolucci et al. (2020), where the variation of Poisson's ratios with respect to wood density are provided for several softwood species, the variation of the Poissons's ratios with W_d can be neglected. Therefore, these quantities are considered constant for both EW and LW phases.

Conformity of the proposed model for the earlywood and latewood phases

The relationships given in Eqs. (11) and (12) to express the dependency of the elastic properties on the relative density (of each phase) must be conform to classical wood behaviour. Guitard (1987) and Cariou (1987) expressed the conformity of wood behaviour through a condition on the ratio between Young's moduli (along different axes) and shear moduli (within different planes), which should be almost constant. The considered ratios are: $\frac{E_{L,k}}{E_{T,k}}$, $\frac{E_{L,k}}{E_{R,k}}$, $\frac{G_{LR,k}}{G_{RT,k}}$, and $\frac{G_{TL,k}}{G_{RT,k}}$.

In this study, a material model is considered conform if all ratios of elastic properties from Eqs. (11) and (12), i.e., $Ra(W_{d,k}) = \frac{E_{L,k}}{E_{T,k}}, \frac{E_{L,k}}{E_{R,k}}, \frac{G_{LR,k}}{G_{RT,k}}, \frac{G_{TL,k}}{G_{RT,k}}$, satisfy the following condition:

$$100\,\frac{|Ra(W_{d,k}) - Ra(0.55)|}{Ra(0.55)} \leq 10\%, \tag{13}$$

where $W_{d,k} \in [0.40, 0.80]$, the mean range of relative densities, with k =EW,LW.

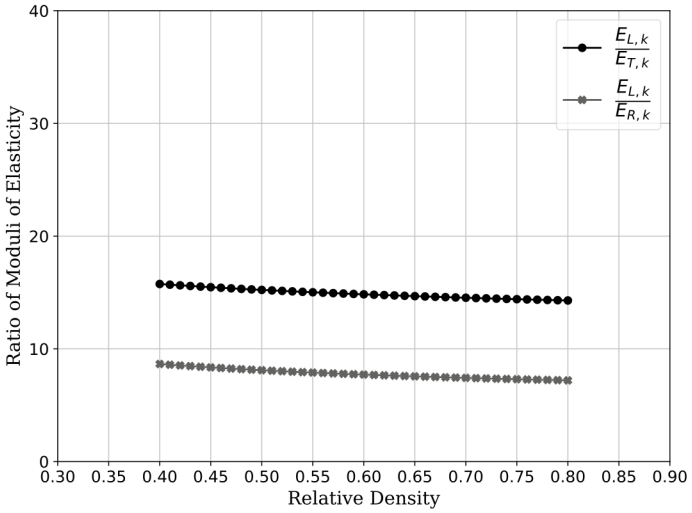

Fig. 3 Young's moduli ratios

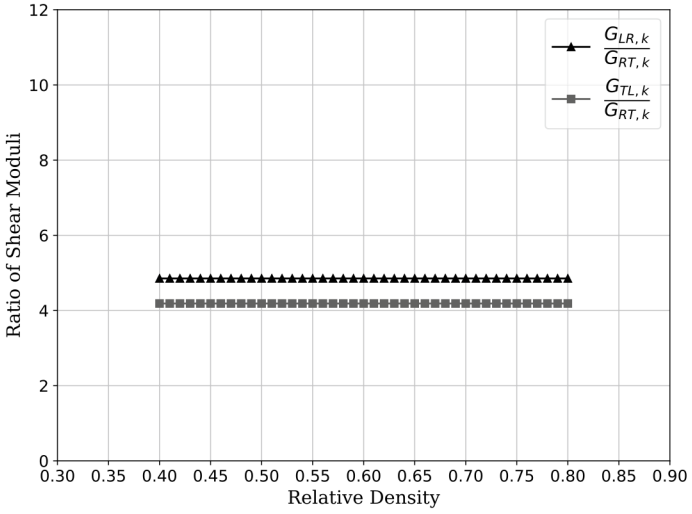

Fig. 4 Shear moduli ratios

Figures 3 and 4 illustrate the elastic properties ratios calculated with the proposed model. All ratios are considered quasi-constant as the condition aforementioned is fulfilled with a maximum variation equal to 7.8%.

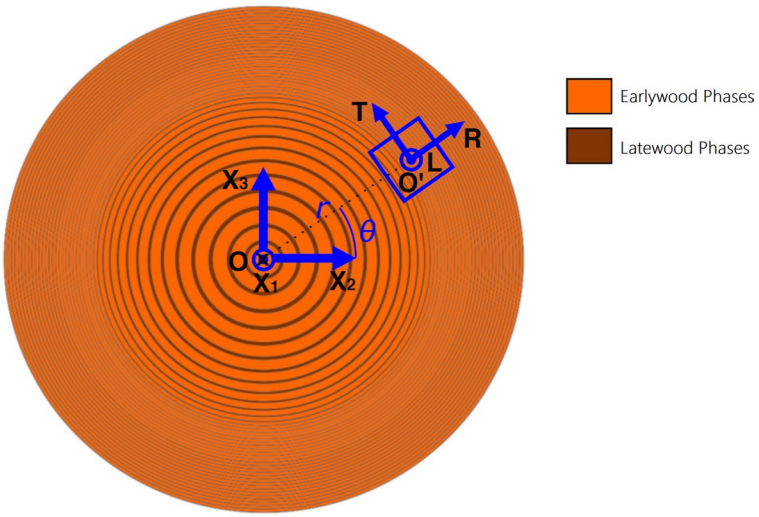

Fig. 5 Main reference systems to describe the position of the RVEs

Determination of the elastic properties at the macroscopic scale

At the microscopic scale, the bibliographic data and the multiple hypotheses introduced on the properties of *Pinus pinaster* (Ait.) allow to propose two different material models for both EW and LW taking into consideration their variability in the stem according to their corresponding relative density.

At the mesoscopic scale, the RVE, which can be seen as a lamellar composite, is modelled by an alternation of constitutive phases, i.e., the EW and LW phases, of varying width and properties to represent the growths rings. The effective properties are determined using the strain energy homogenisation method of periodic media, as presented by Barbero (2008) and extended in Catapano and Jumel (2015) and Delucia et al. (2020). This method is based on the use of periodic boundary conditions (PBCs) and on the postulate that the RVE of a periodic heterogeneous structure and the corresponding volume of a homogeneous solid undergo the same deformation having, hence, the same strain energy. Therefore, the RVEs, which are modelled as lamellar composites, with each layer corresponding to an EW or a LW phase, can be replaced by equivalent homogeneous mediums at the macroscopic scale whose elastic properties and material elastic symmetry are determined through the homogenisation process.

Furthermore, the following assumptions are made to determine the effective properties at the macroscopic scale:

- Linear orthotropic behaviour defined in a local cylindrical reference system for both EW and LW phases;
- Perfect bonding condition at the phases interface is considered.

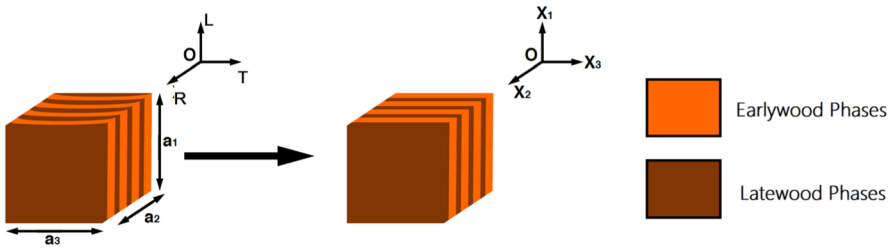

Fig. 6 Constitutive phases of the RVE and transformation from local cylindrical frame to local Cartesian one

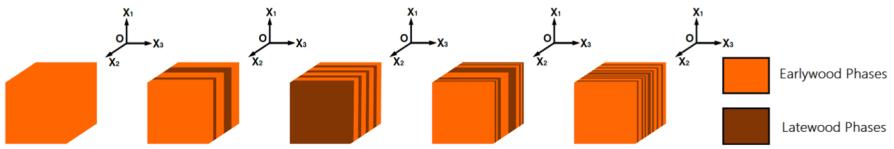

Fig. 7 Examples of RVE configurations in terms of number and width of EW and LW layers, depending on the distance r from the pith

Description of the RVE geometry

The RVEs are extracted from the "synthetic" logs based on the main hypotheses described in Sect. Generation of a synthetic log of *Pinus pinaster* (Ait.). RVEs positions are defined in two main reference systems: a local cylindrical reference system $(O';L,R,T)$ and a global Cartesian reference system $(O;X_1,X_2,X_3)$, defined at the centre of the RVE and the center of the pith, respectively, as shown in Fig. 5.

As this particular homogenisation technique is applied to periodic media and considering the symmetry of the log, RVEs positions are defined solely in terms of distance from the pith r, with respect to the whole synthetic log. Specifically, since the synthetic log geometry (reported in Table 2) and the growth rings geometry are affected by variability, as discussed in Sect. Generation of a synthetic log of *Pinus pinaster* (Ait.), several configurations of RVEs are extracted. These RVEs can vary in terms of number and width of the constitutive rings as a function of the geometry of the synthetic log and of the distance from the pith r. Furthermore, the geometry of EW and LW phases is simplified to straight layers, as illustrated in Fig. 6 where the RVE volume is defined as a parallelepiped in a local Cartesian reference system with a_1, a_2, and a_3 the characteristic lengths of the RVE along the x_1, x_2, and x_3 axes, respectively (which correspond to L, R and T axes in the cylindrical frame). The justification for this simplification is that the size of the RVE at the mesoscopic scale is assumed to be much smaller than the size of the log at the macroscopic scale. Therefore, the curvature of the rings can be disregarded.

Furthermore, since the log geometry and the growth rings geometry are affected by variability, as discussed in Sect. Generation of a synthetic log of *Pinus pinaster* (Ait.), several configurations of RVEs are possible in terms of number and width of the constituting layers, and depending on the distance from the pith r. Indeed in the

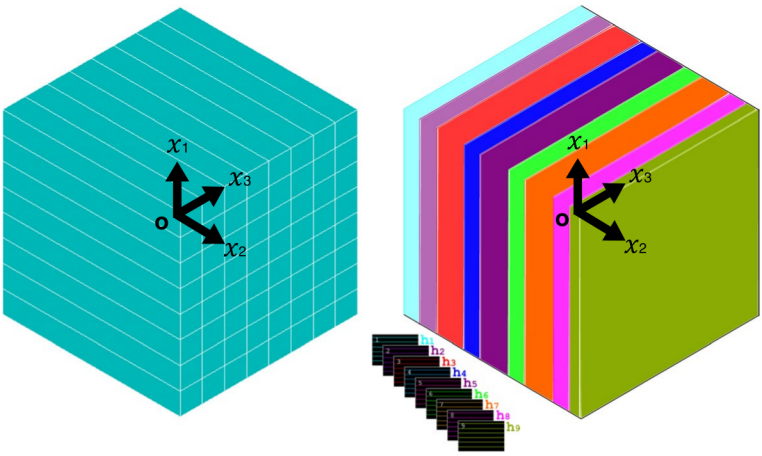

Fig. 8 Finite element model of the RVE modelled as a layered solid (discretised exclusively in (x_1, x_3) plane) and layout of the EW and LW phases having different thickness and material properties along the x_2-axis

RVEs, the number of layers can vary from a single EW layer in the juvenile zone close to the pith to a high number of layers in the adult zone e.g., the RVE in such zone is made of about 8–15 layers as illustrated in Fig. 7.

The finite element model

The geometry used for the generic RVE is shown in Fig. 8. The RVE is a cubic domain modelled as a layered composite, with the axis x_2 perpendicular to the stack made of n_l layers. The geometric parameters are the side of the cubic RVE, i.e., $a_1 = a_2 = a_3 = h$, the distance from the pith of the centroid of the RVE r, and the thickness of each rectangular parallelepiped layer modelling the EW and LW phases in the RVE, i.e., h_j with $j = 1, ..., n_l$. Specifically, the volume of the RVE is always the same and defined as $V_{\text{RVE}} = h^3$. Of course, the relationship between the side of the cube and the thickness of the layers is:

$$h = \sum_{j=1}^{n_l} h_j, \tag{14}$$

where $n_l = n_l\left(h, r, \text{RW}_i, \text{LWP}_i\right)$ and $h_j = h_j\left(h, r, \text{RW}_i, \text{LWP}_i\right)$ are the number of layers and thickness of the layers composing the RVE, respectively, that depend on the dimension of the cube side h, the distance r, and the rings geometry parameters RW_i and LWP_i. The expression of RW_i and LWP_i are provided in Eqs. (3) and (4).

The RVEs are extracted from the synthetic logs (described in Sect. Generation of a synthetic log of *Pinus pinaster* (Ait.) which are generated thanks to a parametric script coded in Python® environment by considering the variability on the quantities introduced in Sect. Generation of a synthetic log of *Pinus pinaster* (Ait.). The parametric FE model is then created within the commercial FE code Ansys®. 20-node solid elements (SOLID186) with three Degrees of Freedom (DOFs) per node have been

used. The "Layered" option has been activated to model each phase of EW and LW as an equivalent layer with 3 integration points per layer. When using this option, the Reissner-Mindlin kinematic model is activated through the thickness of the layered solid (ANSYS, Inc. 2013), i.e., along axis x_2 by referring to Fig. 8. According to "Layered" option, the RVE discretisation is possible exclusively in (x_1, x_3) plane. No discretisation along x_2 direction (i.e. the rings width direction) is possible.

The choice of using a numerical homogenisation strategy, based on the FE method, instead of an analytical one based on well-established theories like CLPT or Fist-order Shear Deformation Theory (FSDT) is related to the need of a correct evaluation of the stress field into each layer (i.e. the EW and LW phases) constituting the RVE. Since the goal of this paper is to determine the effective properties of *Pinus pinaster* (Ait.) accounting for variability, an efficient numerical strategy is needed to obtain a good balance between accuracy and computational effort. To this end, the FSDT enhanced with a correction of the stress field implemented in the SOLID186 element of ANSYS software is used. Specifically, in its layered version, this element integrates a correction of the stress field within each layer, which is determined during post-processing operations as a solution of the local equilibrium equation.

The numerical homogenisation method

In the following, the strain energy homogenisation technique of periodic media (Barbero 2008) is briefly recalled. This technique is based on the assumption that the RVE of the periodic heterogeneous medium and the corresponding equivalent homogeneous solid undergo the same total strain energy. In the 3D case, the generalized Hooke's law for the equivalent elastic material at the upper scale can be written under the form:

$$\overline{\sigma}_i = \overline{C}_{ij}\overline{\varepsilon}_j \; i,j = 1,\ldots,6, \tag{15}$$

where $\overline{\sigma}$ and $\overline{\varepsilon}$ are the volume-averaged components of the stress and strain tensors expressed in Voigt's notation, respectively, of the equivalent homogeneous anisotropic continuum, whereas $\overline{C}_{ij}$ are the components of the homogenised stiffness matrix of the RVE.

In order to evaluate the components of the stiffness matrix $\mathbf{C}$ of the generic RVE at the macroscopic scale, the RVE is submitted to a mono-axial strain field $\overline{\varepsilon}^0_{ij}$, with $i,j = 1,2,3$ (tensor notation). The six independent components of the strain vector are applied by considering the following set of PBCs, (Barbero 2008):

$$\begin{cases} u_i(a_1/2,x_2,x_3) - u_i(-a_1/2,x_2,x_3) = a_1\overline{\varepsilon}^0_{i1}, \;\; (-a_2/2 \le x_2 \le a_2/2, \; -a_3/2 \le x_3 \le a_3/2), \\ u_i(x_1,a_2/2,x_3) - u_i(x_1,-a_2/2,x_3) = a_2\overline{\varepsilon}^0_{i2}, \;\; (-a_1/2 \le x_1 \le a_1/2, \; -a_3/2 \le x_3 \le a_3/2), \\ u_i(x_1,x_2,a_3/2) - u_i(x_1,x_2,-a_3/2) = a_3\overline{\varepsilon}^0_{i3}, \;\; (-a_1/2 \le x_1 \le a_1/2, \; -a_2/2 \le x_2 \le a_2/2), \end{cases} \tag{16}$$

where $i = 1,2,3$, while a_i is the characteristic length of the RVE along the x_i axis.

After solving the linear static analysis for each load case, it is possible to recover the components of the volume-averaged stress vector, i.e., $\overline{\sigma}_\alpha$ with $\alpha = 1,\ldots,6$:

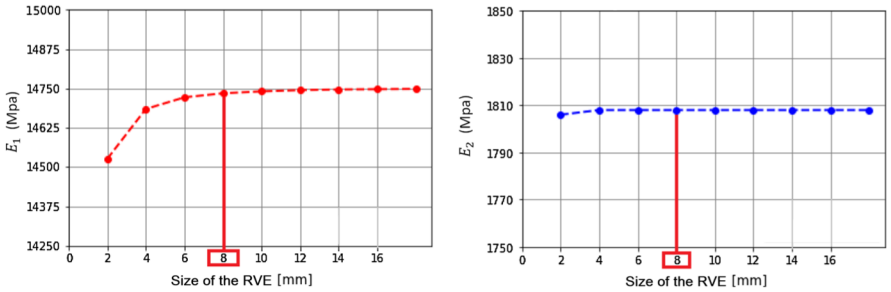

Fig. 9 Effective Young's moduli vs. RVE size

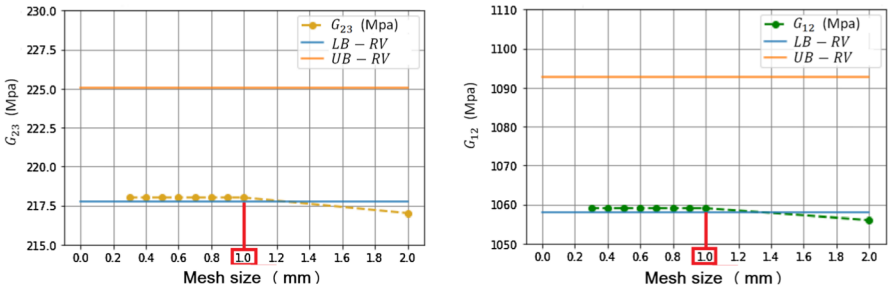

Fig. 10 Effective shear moduli vs. mesh size. LB-RV (Lower bound of Reuss-Voigt), UB-RV (Upper bound of Reuss-Voigt)

$$\begin{aligned}\bar{\sigma}_\alpha\left(x_1,x_2,x_3\right) &= \frac{1}{V_{\text{RVE}}}\int_{V_{\text{RVE}}}\sigma_\alpha\left(x_1,x_2,x_3\right)dV \\ &\approx \frac{1}{V_{\text{RVE}}}\sum_{e=1}^{N_e}\sum_{j=1}^{n_l}\sigma_{\alpha ej}\left(x_1,x_2,x_3\right)A_{ej}h_j,\end{aligned} \tag{17}$$

where A_{ej} is the area of the j-th layer of element e, whilst N_e is the number of elements composing the mesh of the FE model of the RVE.

The components $\overline{C}_{\alpha\beta}$ of the stiffness matrix at the upper scale are determined column-wise by applying the PBCs of Eq. (16) and elementary uniaxial strain fields. This operation results in six static analyses wherein only one component $\overline{\varepsilon}_\beta$ of the strain vector is different from zero, i.e.,

$$\overline{C}_{\alpha\beta} = \frac{\overline{\sigma}_\alpha}{\overline{\varepsilon}_\beta} \text{ with } \alpha,\beta = 1,...,6 \text{ and } \overline{\varepsilon}_\gamma = 0 \text{ with } \gamma = 1,...,6 \text{ and } \gamma \neq \beta. \tag{18}$$

Finally, to check the positive definiteness of the stiffness tensors at the upper scale, the set of the effective elastic constants resulting from the numerical homogenisation $\mathcal{M} := \{E_1, E_2, E_3, G_{12}, G_{23}, G_{13}, \nu_{21}, \nu_{23}, \nu_{31}\}$ have to satisfy the following set of inequalities (Cappelli et al. 2018):

$$
\begin{aligned}
&g_1(\mathcal{M}) = -E_1 \leq 0,\\
&g_2(\mathcal{M}) = -E_2 \leq 0,\\
&g_3(\mathcal{M}) = -E_3 \leq 0,\\
&g_4(\mathcal{M}) = -G_{12} \leq 0,\\
&g_5(\mathcal{M}) = -G_{23} \leq 0,\\
&g_6(\mathcal{M}) = -G_{31} \leq 0,\\
&g_7(\mathcal{M}) = |\nu_{23}| - \sqrt{\frac{E_2}{E_3}} < 0,\\
&g_8(\mathcal{M}) = |\nu_{31}| - \sqrt{\frac{E_3}{E_1}} < 0,\\
&g_9(\mathcal{M}) = |\nu_{12}| - \sqrt{\frac{E_1}{E_2}} < 0,\\
&g_{10}(\mathcal{M}) = 2\nu_{23}\nu_{31}\nu_{12} + {\nu_{23}}^2\frac{E_3}{E_2}\\
&+{\nu_{31}}^2\frac{E_1}{E_3} + {\nu_{12}}^2\frac{E_2}{E_1} - 1 < 0,\\
&g_{11}(\mathcal{M}) = \nu_{23} + \nu_{31} + \nu_{12} - \frac{3}{2} < 0.
\end{aligned}
\tag{19}
$$

Numerical results at the macroscopic scale accounting for variability

Convergence analyses

To validate the accuracy and effectiveness of the FE model of the RVE, the sensitivity analyses of the results to the RVE size and the mesh size are realised exclusively in terms of mean values of physical and geometrical parameters (no variability is taken into account in this preliminary study), as shown in Figs. 9 and 10.

The convergence analyses are performed in the adult zone due to the higher number of layers composing the cubic RVE (whose edge length is $a_1 = a_2 = a_3 = h$) in this region. The obtained results are considered valid on the whole range of r.

According to the main results presented in Figs. 9 and 10, for a RVE size of $h = 8$ mm, the best compromise in terms of computational costs and accuracy in terms of elastic constants is a mesh size equal to $e_{\text{size}} = \frac{h}{8}$. The computational time for one simulation is equal to approximately 3.0 seconds on a personal computer with an Intel® Core™ i7-7700K CPU @ 4.20GHz processor with 16.0 GB of RAM.

Monte-Carlo method

The Monte-Carlo (*MC*) method is commonly used to estimate the probabilistic distribution of simulation results and it has already been used in the case of natural materials, such as cork agglomerates (Delucia et al. 2020). In this study, the variability induced by the proposed model on the RVEs configuration, i.e., number of layers composing the RVE, their width, their elastic properties, and their composition,

which depend on the distance from the pith r, influences the resulting effective mechanical properties at the macroscopic scale. This influence can be assessed thanks to the MC method coupled with the numerical homogenisation technique described in Sect. Determination of the elastic properties at the macroscopic scale. The MC method applied in this study relies on four main steps:

- Step 1. The parametric FE model takes into consideration the variability of each input parameter, as presented in Sect. Generation of a synthetic log of *Pinus pinaster* (Ait.).
- Step 2. A statistically representative number of samples is chosen by performing a convergence analysis to obtain information on the studied population of RVEs.
- Step 3. The homogenisation process is carried out for each RVE sample to obtain the probabilistic distribution of the equivalent elastic properties at the macroscopic scale at a given distance from the pith r.
- Step 4. Steps 1-3 are repeated for values of r in the range $r \in [4, 150]$ mm with an increment of 1 mm.

The number of samples n used in this study has been estimated by analysing the convergence of equivalent elastic properties mean and standard deviation of RVEs over the whole range of r. For the sake of brevity, this convergence analysis is not presented here, while only the results are given. The number of samples to be analysed is equal to $n = 250$, which means that n homogenisation analyses are performed for each value of r in the selected range (Steps 3 and 4).

Numerical results

To show the effectiveness of the proposed approach, a comparison between the proposed numerical model and the variational bounds of Reuss-Voigt (R-V) over the range of interest of the variable r is performed. Furthermore, experimental data taken from the literature are juxtaposed to the results as further comparison term. These data are taken from various studies, such as Cariou (1987); Pereira et al. (2014) and Santos (2007). Moreover, additional data are introduced from Morgado et al. (2011, 2017); Pedro (2013) and Carballo et al. (2009), who evaluated the longitudinal modulus of elasticity with 4-points bending tests reposing on several European standards adopted as French standards in AFNOR (2004, 2012, 2022) (for local and global longitudinal Young's modulus).

Moreover, the results obtained for the mean value and 68% confidence interval of the set of equivalent elastic properties $E_1, E_2, E_3, G_{12}, G_{23}, G_{31}$ of the layered composite at the macroscopic scale over the range $r \in [4, 150]$ mm are shown in Figs. 11 and 12.

The mean values of the effective elastic properties as well as the confidence intervals always fall within the variational analytical R-V bounds. Thus, the validity of the numerical method is verified.

It is noteworthy that there is relatively few literature information concerning all the elastic properties except the longitudinal Young's modulus $E_1 = E_L$. Moreover,

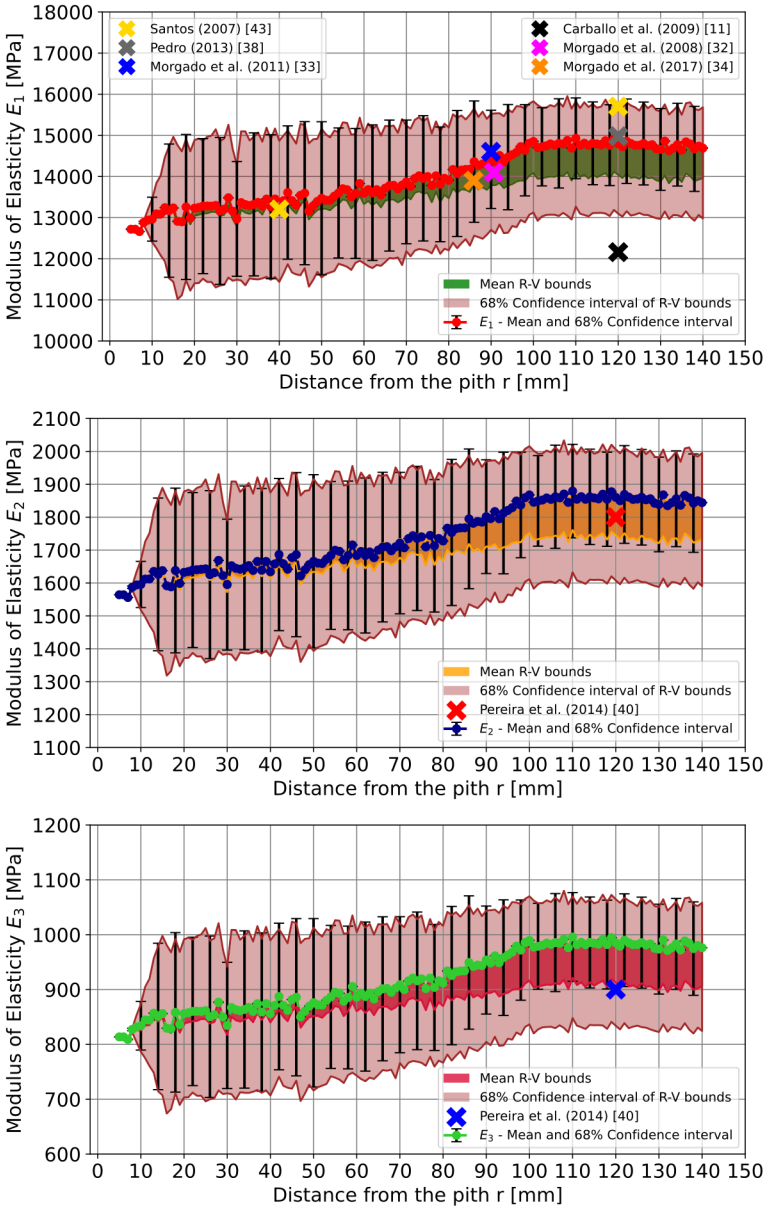

Fig. 11 Effective Young's moduli vs. distance from the pith with the associated variability. Experimental values are placed at the corresponding model densities. Relative densities are included in [0.46; 0.60]–unknown for (Pereira et al. 2014)

the overall data on *Pinus pinaster* (Ait.) comes from Portugal where the trees tend to have an overall higher density. Nonetheless, the model results seem in good

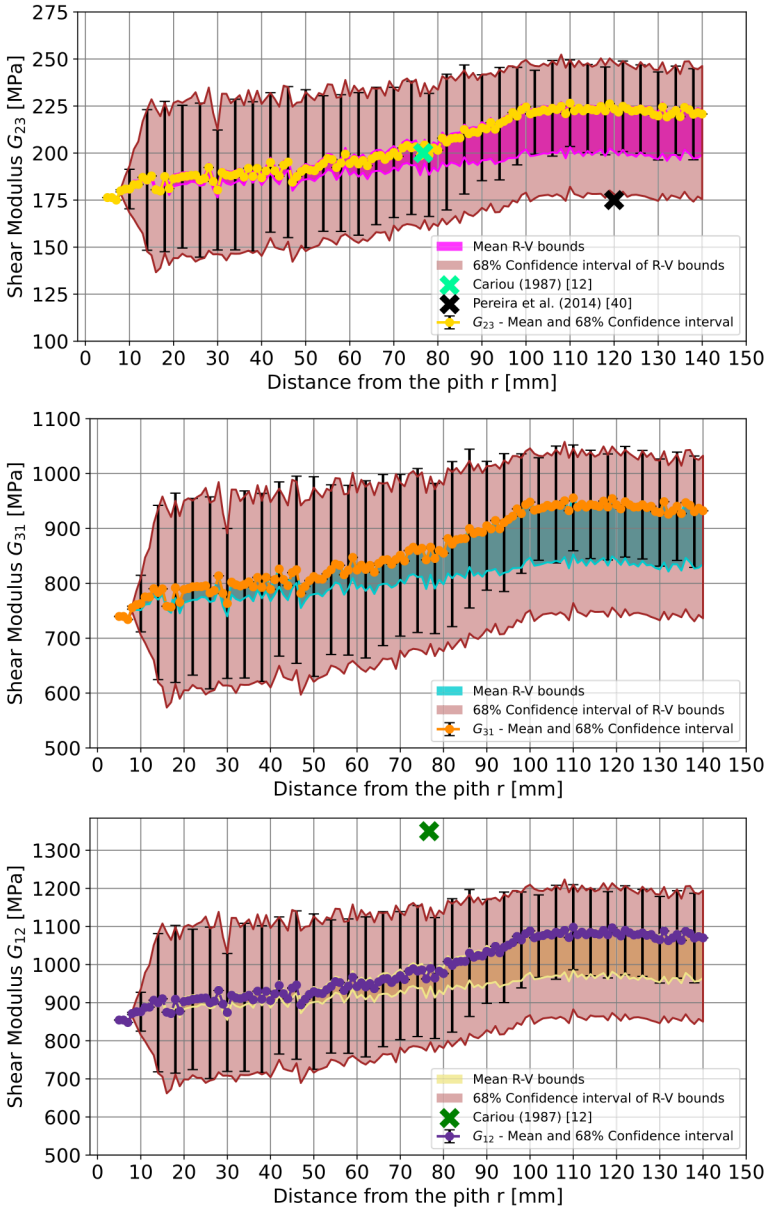

Fig. 12 Effective shear moduli vs. distance from the pith with the associated variability. Experimental values are placed at the corresponding model densities. Relative density is 0.51 for (Cariou 1987) and unknown for (Pereira et al. 2014)

agreement with the experimental data obtained from the scientific literature, which are almost all included into the 68% confidence interval.

Table 6 Effective Poisson's ratios obtained from the numerical study and similar to the entry data with k=EW,LW

$\nu_{23} = \nu_{RT,k}$	$\nu_{31} = \nu_{TL,k}$	$\nu_{21} = \nu_{RL,k}$
0.58	0.03	0.04

As shown in Figs. 11 and 12, the set of elastic properties increases with the distance from the pith with important variations in the juvenile zone, i.e., $r \in [20, 100]$ mm. Conversely, when $r > 100$ mm, as the adult zone is reached, the elastic properties tend to stabilise around an horizontal asymptote. These observations are consistent with the hypotheses on the input physical parameters provided in Sect. Generation of a synthetic log of *Pinus pinaster* (Ait.). Finally, the values for the Poisson's ratios are always constant, equal to the input properties, and presented in Table 6.

Variability estimation

Experimental data taken from Santos et al. (2008); Morgado et al.(2008, 2011, 2017); Pereira et al. (2014) and Carballo et al. (2009) are available to estimate the overall variability of elastic properties and density across whole trunks of *Pinus pinaster* (Ait.). Nevertheless, to correctly compare the numerical results of the present work with those available in the literature, which have been obtained for different values of $r \in [50, 140]$ mm, a unique mean value of elastic constants with the associated coefficient of variation $C_v(M)$, calculated from Eq. (2), is determined. To this end, $N_{cv} = 10^6$ values of elastic properties have been randomly picked for $r \in [50, 140]$ mm by considering the plots in Figs. 11 and 12. Then, the mean value and the coefficient of variation of each effective elastic property have been determined. Table 7 presents the differences between the numerical results obtained with the present methodology and the experimental results available in the literature. Moreover, for the sake of brevity, only the coefficients of variation of E_1 and G_{12} are illustrated in Fig. 13. The coefficients of variation of the other elastic properties exhibit a similar trend.

From the analysis of these results, one can notice that the variation of density considered in this study is higher than that of the experimental data, as the variability across the whole (R, T) plane of the synthetic log is considered in the proposed modelling strategy. However, in the case of the Young's moduli, the coefficients of variation obtained numerically are lower than the experimental counterpart. This is due to the simplifying hypotheses introduced on log shape, reaction wood, longitudinal variability, which, coupled with the linear relationship between elastic properties and density, lead to an underestimation of the elastic properties variability.

Table 7 Comparison between numerical and experimental values of elastic properties and density (with the associated coefficients of variation)

Source	$\mathbf{E_1}$ [MPa]	$\mathbf{C_v(E_1)}$ [%]	$\mathbf{E_2}$ [MPa]	$\mathbf{C_v(E_2)}$ [%]	$\mathbf{E_3}$ [MPa]	$\mathbf{C_v(E_3)}$ [%]	$\mathbf{W_d}$	$\mathbf{C_v(W_d)}$
Proposed model	13955	11.1	1737.7	12.8	915.87	14.0	0.556	24.1
Table 2 Pereira et al. (2014)	–	–	1800	12.8	900	23.7	–	–
Table 2 Carballo et al. (2009)	12161	21	–	–	–	–	0.573	11
Table 2 Morgado et al. (2017)	13900	17.96	–	–	–	–	0.5288	9.64
Table 3 Morgado et al. (2011)	14600	23.3	–	–	–	–	0.535	11
Table 1 Santos et al. (2008)	15100	6.8	1910	7.9	1010	14.4	–	–

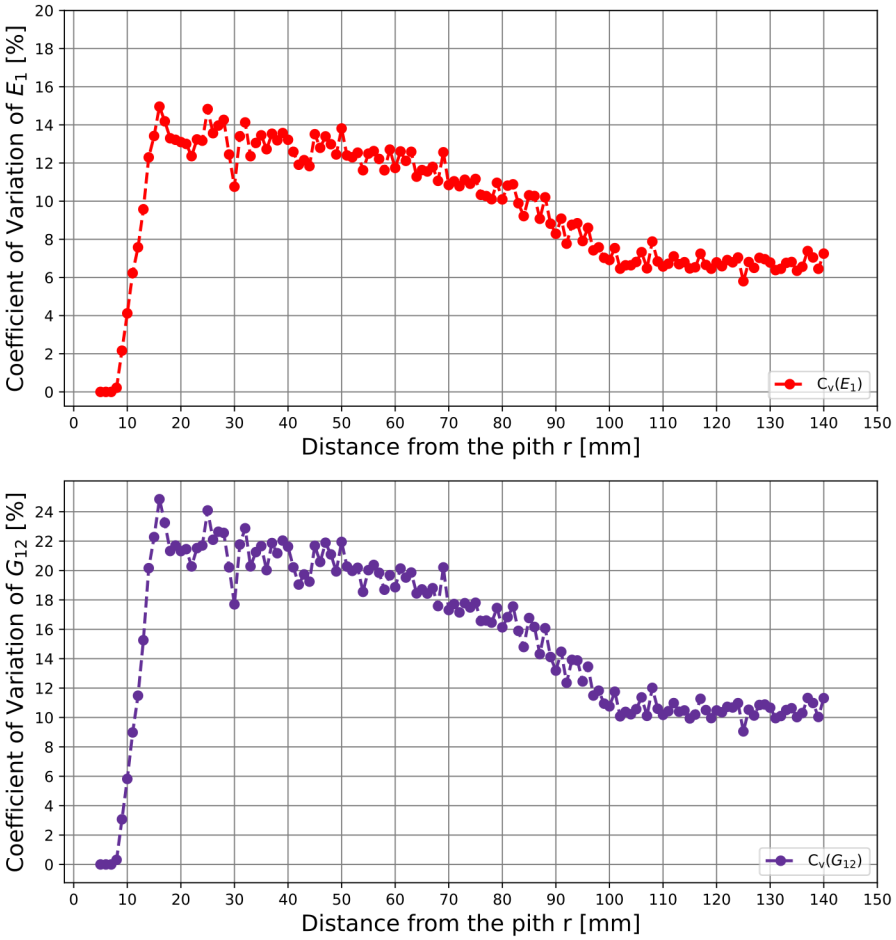

Fig. 13 Effective coefficient of variation [%] vs. the distance from the pith

Conclusion

A multi-scale modelling strategy to determine the elastic properties of *Pinus pinaster* (Ait.) taking into consideration the associated variability has been proposed in this work. The proposed modelling strategy is articulated in different steps.

Firstly, at a length scale of hundreds of micrometres, a parametric model has been coded on Python® environment to generate a database of EW and LW properties resting on experimental data, taken from the scientific literature. Secondly, the well-known strain energy homogenisation method of periodic media has been used on a numerical model at the mesoscopic scale, i.e., at a length scale of millimetres, to

determine the macroscopic equivalent elastic behaviour of small samples of *Pinus pinaster* (Ait.). Both models take into consideration the heterogeneity and variability of main wood properties at the microscopic scale (intra-ring) and at the mesoscopic scale (inter-rings). The RVE of the mesoscopic scale model is composed of several rings, each one modelled through two constitutive phases, i.e., EW and LW. The EW and LW phases of the RVE are modelled in a layered solid element whose layer thickness and material properties are different and depend on the distance from the pith. The Monte Carlo algorithm is used to account for the variability of the different geometric and material properties involved in the definition of the RVE and to realise statistical analyses on the equivalent elastic properties. These analyses are conducted to understand the propagation of the variability across the scales. Normal probability density functions have been considered to represent the overall behaviour of wood physical parameters. In order to show the effectiveness of the modelling strategy, equivalent elastic properties are compared with analytical results as well as experimental data extracted from the scientific literature. Numerical results fall within the range of the upper and lower variational bounds of Reuss and Voigt and mean values are in agreement with experimental results. Nonetheless, their overall variation seems to be underestimated by the proposed model due to the adopted simplifying hypotheses. Moreover, the influence of distance from the pith on the elastic properties is investigated. The elastic properties undergo a significant increment in the juvenile wood before reaching a limit value in the adult zone. This result is in agreement with trends provided in the literature.

As far as prospects of this work are concerned, it is necessary to further generalise this model to improve its accuracy by relaxing some simplifying hypotheses, such as the perfect circular shape of the trunk and rings, the absence of reaction wood, knots and longitudinal variability.

Funding Gascogne Bois and ANRT, supporting the first author through *Thèse CIFRE* Grant 1264, are gratefully acknowledged.

Data availibility The raw/processed data required to reproduce these findings cannot be shared at this time as the data also forms part of an ongoing study.

Declarations

Conflict of interest The authors declare that they have no known competing financial interests or personal relationships that could have appeared to influence the work reported in this paper.

References

AFNOR (2004) NF EN 14251 : Bois de structure rond–Méthodes d'essai, [NF EN 14251 : Circular structural wood–Test methods]

AFNOR (2012) NF EN 408+A1 : Structures en bois–Bois de structure et bois lamellé-collé–Détermination de certaines propriétés physiques et mécaniques, [NF EN 408+A1 : Wood structures–Structural wood and glued lamelled timbers]

AFNOR (2022) NF EN 384+A2 : Bois de structure–Détermination des valeurs caractéristiques des propriétés mécaniques et de la masse volumique, [NF EN 384+A2 : Stuctural wood–Determination of mechanical properties and density]

Alazwari M, Rao S (2019) Modeling and analysis of composite laminates in the presence of uncertainties. Compos B Eng 161:107–120

ANSYS, Inc (2013) ANSYS Mechanical APDL Basic Analysis Guide. Release 15.0. Southpointe, 275 Technology Drive, Canonsburg, PA 15317

Barbero E (2008) Finite element analysis of composite materials. CRC Press–Edition Taylor and Francis Group

Bartolucci B, De Rosa A, Bertolini C, Berto F, Penta F, Siani A (2020) Mechanical properties of the most common european woods: a literature review. Frattura ed Integrità Strutturale 54:249–274

Berthier B, Kokutse A, Stokes A, Fourcaud T (2001) Irregular Heartwood Formation in Maritime Pine (Pinus pinaster Ait): consequences for biomechanical and hydraulic tree functioning. Ann Bot 87(1):19–25

Brémaud I, Ruelle J, Thibaut A, Thibaut B (2013) Changes in viscoelastic vibrational properties between compression and normal wood: roles of microfibril angle and of lignin. Holzforschung 67(1):75–85

Cappelli L, Montemurro M, Dau F, Guillaumat L (2018) Characterisation of composite elastic properties by means of a multi-scale two-level inverse approach. Compos Struct 204:767–777

Carballo J, Hermoso E, Fernández-Golfín J (2009) Mechanical properties of structural maritime pine sawn timber from Galicia (Pinus pinaster Ait. ssp. atlantica). Investigación Agraria: Sistemas y Recursos Forestales 18(2):152–158

Cariou JL (1987) Caractérisation d'un matériau viscoélastique anisotrope: le bois, [Characterisation of a viscoelastic anisotropic material: the wood]. PhD thesis, Université Bordeaux I

Catapano A, Jumel J (2015) A numerical approach for determining the effective elastic symmetries of particulate-polymer composites. Compos B Eng 78:227–243

Chen S, Wei Y, Wang G, Zhao K, Ding M (2023) Mechanical behavior of laminated bamboo-timber composite columns under axial compression. Archiv. Civ. Mech. Eng. 23:72

Chevalier R, Catapano A, Pommier R, Montemurro M (2024) A review on properties and variability of Pinus Pinaster Ait. ssp. Atlantica existing in the Landes of Gascogne. J Wood Sci 70(14):1–25

Cramer S, Kretschmann D, Lakes R, Schmidt T (2005) Earlywood and latewood elastic properties in loblolly pine. Holzforschung 59:531–538

Delucia M, Catapano A, Montemurro M, Pailhés J (2020) A stochastic approach for predicting the temperature-dependent elastic properties of cork-based composites. Mech Mater 145:103399

Einstein A (1905) Über die von der molekularkinetischen Theorie der Wärme geforderte Bewegung von in ruhenden Flüssigkeiten suspendierten Teilchen, [About the movement of particles suspended in liquids at rest as required by the molecular kinetic theory of heat]. Ann Phys 322(8):549–560

Fabrizio C, Sciomenta M, Spera L, De Santis Y, Pagliaro S, Di Egidio A, Fragiacomo M (2023) Experimental investigation and beam-theory-based analytical model of cross-laminated timber panels buckling behavior. Archiv Civ Mech Eng 23:172

FPL–Forest Products Laboratory (2010) Wood Handbook, Wood as an Engineering Material. General Technical Report FPL-GTR-190, U.S. Departement of Agriculture, Forest Service, Madison

Gaspar M, Louzada J, Silva M, Aguiar A, Almeida M (2008) Age trends in genetic parameters of wood density components in 46 half-sibling families of Pinus pinaster. Can J For Res 39(6):1470–1477

Ghoroubi R, Mercimek O, Sakin S, Anil O (2022) Experimental investigation of bonding behavior of anchoraged timber-to-timber joint. Archiv Civ Mech Eng 22:7

Girardon S, Denaud L, Pot G, Rahayu I (2016) Modelling the effects of wood cambial age on the effective modulus of elasticity of poplar laminated veneer lumber. Ann Sci 73(3):615–624

Guitard D (1987) Mécanique du matériau bois et composites–préface [Material mechanics for wood and composites–préface] of H. Polge

Hashin Z, Shtrikman S (1962) A variational approach to the theory of the elastic behaviour of multiphase materials. J Mech Phys Solids 11(2):127–140

Hofstetter K, Hellmich C, Eberhardsteiner J (2005) Development and experimental validation of a continuum micromechanics model for the elasticity of wood. Eur J Mech A Solids 24(6):1030–1053

IPCC 2014 (2014) Climate Change 2014: Mitigation of Climate Change. Contribution of Working Group III to the Fifth Assessment Report of the Intergovernmental Panel on Climate Change [Edenhofer O. and Pichs-Madruga, R. and Sokona, Y. and Farahani, E. and Kadner, S. and Seyboth, K. and Adler, A. and Baum, I. and Brunner, S. Eickemeier, P. and Kriemann, B. and Savolainen, J. and

Schlömer, S. and von Stechow, C. and Zwickel, T. and Minx, J.-C. (eds.)]. Tech. rep., IPCC: Intergovernmental Panel on Climate Change, Cambridge, United Kingdom and New York, NY, USA

IPCC 2018 (2018) Global Warming of 1.5°C. An IPCC Special Report on the impacts of global warming of 1.5°C above pre-industrial levels and related global greenhouse gas emission pathways, in the context of strengthening the global response to the threat of climate change, sustainable development, and efforts to eradicate poverty [Masson-Delmotte V. and Zhai, P. and Pörtner, H.O. and Roberts, D. and Skea, J.. and Shukla, P.R. and Pirani, A. and Moufouma-Okia, W. and Péan, C. Pidcock, R. and Connors, S. and Matthews, J.B.R. and Chen, Y. and Zhou, X. and Gomis, M.I.. and Lonnoy, E. and Maycock, T. and Tignor, M. and Waterfield, T. (eds.)]. Tech. rep., IPCC: Intergovernmental Panel on Climate Change, Cambridge, United Kingdom and New York, NY, USA

Jodin P, Militon J (1994) Le bois matériau d'ingénierie [Wood as an engineering material] by Philippe Jodin. Association pour la recherche sur le bois en Lorraine école nationale du génie rural, des eaux et des forêts [Association for Wood Research in Lorraine école nationale du génie rural, des eaux et des forêts], Nancy

Kasal B (2004) Wood formation and properties–Mechanical Properties of Wood. In: Press A (ed) Encyclopedia of Forest Sciences, pp 1815–1828

Kokutse A, Berthier S, Stokes A (1999) Formation et développement du bois de cœur, [Forming and developing heartwood]. In: Editions ARBORA (ed) Castéra P, ed. Propriétés et usages du Pin maritime [Properties and use of Maritime Pine], Bordeaux, pp 287–290

Lahna F (1983) Mécanique de la rupture des matériaux orthotropes-Application au bois [Fracture mechanics of orthotropic materials–Application to wood]. PhD thesis, Université Bordeaux I

Louzada J (2003) Genetic correlations between wood density components in Pinus pinaster Ait. Ann For Sci 60(3):285–294

McManus H (1993) Probabilistic methods for the calculation of laminate properties. J Reinf Plast Compos 12(6):712–722

Moreau J (2010) Impact de pratiques sylvicoles intensives sur les propriétés du bois de pin maritime [Impact of intensive silvicultural practices on the properties of maritime pine wood]. PhD thesis, Université Bordeaux I, http://www.theses.fr/2010BOR14200

Morgado T, Rodrigues J, Saporiti J, Dias A (2008) Grading and testing of Maritime pine and larch Roundwood. In: Conference COST E53, Delft, The Netherlands

Morgado T, Machado J, Dias A, Cruz H, Rodrigues J (2011) Características mecânicas et classifição da madeira de secção circular de Pinheiro Bravo [Mechanical characteristics and classification of Pinheiro Bravo circular-sectioned wood]. In: CIMAD 11 -1° Congresso Ibero-LatinoAmericano da Madeira na Construção [1° Ibero-Latin American Congress on Wood in Construction], Coimbra, Portugal

Morgado T, Dias A, Machado J, Negrao J, Marques A (2017) Grading of Portuguese maritime pine small-diameter roundwood. J Mater Civ Eng 29(2):04016209

Moutee M (2006) Modélisation du comportement mécanique du bois au cours du séchage [Modelling the mechanical behaviour of wood during drying]. PhD thesis, Université de Laval, Québec

Niccoli F, Esposito A, Altieri S, Battipaglia G (2019) Fire severity influences ecophysiological responses of pinus pinaster Ait. Front Plant Sci 10:539

Nicholls J, Dadswell H, Perry D (1963) Assessment of wood qualities for tree breeding. II. In Pinus Pinaster Ait. from Western Australia. Silvae Genetica 12(4):105–110

Pedro J (2013) Avaliação destrutiva e não destrutiva de elementos retangulares de madeira de pinho bravo [Destructive and non-destructive evaluation of rectangular Pinus pinaster wood elements]. Master's thesis, Faculdade de Ciências e Tecnologia da Universidade de Coimbra, Portugal

Pereira J (2005) Comportamento mecânico da madeira em tracção nas direcções de simetria material [Mechanical behaviour of wood in traction in directions of material symmetry]. Master's thesis, Universidade de Tràs-os-Montes e Alto Douro, Vila Real, Portugal

Pereira J, Xavier J, Morais J, Louzada J (2014) Assessing wood quality by spatial variation of elastic properties within the stem: case study of Pinus pinaster in the transverse plane1. Can J For Res 44(2):107–117

Plomion C, Pionneau C, Brach J, Costa P, Baillères H (2000) Compression wood-responsive proteins in developing xylem of maritime pine (Pinus pinaster Ait.). Plant Physiol 123(3):959–970

Qing H, Mishnaevsky L (2010) 3d multiscale micromechanical model of wood: from annual rings to microfibrils. Int J Solids Struct 47(9):1253–1267

Reuss A (1929) Berechnung der Fließgrenze von Mischkristallen auf Grund der Plastizitätsbedingung für Eisnkristalle [Calculation of the flow limit of solid solutions based on the plasticity condition for single crystals]. J Appl Math Mech 9(1):49–58

Saavedra Flores E, Saavedra K, Hinojosa J, Chandra Y, Das R (2016) Multi-scale modelling of rolling shear failure in cross-laminated timber structures by homogenisation and cohesive zone models. Int J Solids Struct 81:219–232

Santos C, De Jesus A, Morais J, Louzada J (2008) Bearing properties of portuguese pine wood beneath a laterally loaded dowel. Ciência e Tecnologia dos Materiais 20(1–2):45–51

Santos J (2007) Estudo de Modelos e Caracterização do Comportamento Mecânico da Madeira [Study of Models and Characterisation of the Mechanical Behaviour of Wood]. PhD thesis, Universidade do Minho

Sanz F, Latour S, Neves M, Bastet E, Pischedda D, Piñeiro G, Gauthier T, Lesbats J, Plantier C, Marques A, Lanvin JD, Santos J, Touza M, Pedras F, Parrot J, Reuling D, Faria C (2020) Industrial applications of Pinus Pinaster. Center of Innovations and Technological Services of Madeira in Galicia, founded by development of technological industrial quality ofGalicia edition, Madeira, Spain

Sejnoha M, Kucíková L, Vorel J, Sýkora J, De Wilde W (2019) Effective material properties of wood based on homogenization. Int J Comput Methods Exper Measure 7(2):167–180

Sejnoha M, Sýkora J, Vorel J, Kucíková L, Antoš J, Pokorný J, Pavlík Z (2019) Moisture induced strains in spruce from homogenization and transient moisture transport analysis. Comput Struct 220:114–130

Sun X, He M, Li Z (2022) Experimental investigation on the influence of lamination aspect ratios on rolling shear strength of cross-laminated timber. Archiv Civ Mech Eng 22:22

Taylor A, Gartner B, Morrell J (2002) Heartwood formation and natural durability-a review. Wood Fiber Sci 34(4):587–611

Voigt W (1889) Ueber die Beziehung zwischen den beiden Elasticitätsconstanten isotroper Körper [About the relationship between the two elasticity constants of isotropic bodies]. Ann Phys 274(12):573–587

Xavier J (2003) Caracterização do comportamento ao corte da madeira usando o ensaio de Iosipescu [Characterisation of the cutting behaviour of wood using the Iosipescu test]. Master's thesis, Dissertação de Mestrado em Tecnologias das Engenharias [Master's Degree in Engineering Technologies], Universidade de trás-os-montes e alto douro, Vila Real

Xavier J, Garrido N, Oliveira M, Morais J, Camanho P, Pierron F (2004) A comparison between the Iosipescu and off-axis shear test methods for the characterization of Pinus Pinaster Ait. Compos A Appl Sci Manuf 35(7–8):827–840

Xavier J, Oliveira M, Morais J, Pinto T (2009) Measurement of the shear properties of clear wood by the Arcan test. Holzforschung 63(2):217–225

Zobel B, Sprague J (1998) Juvenile Wood in Forest Trees. Springer Berlin, Heidelberg. ISSN: 1431-8563